

## DETERMINATION OF JOHNSON-COOK EQUATION PARAMETERS

M. Šlais<sup>1)\*</sup>, I. Dohnal<sup>1)</sup>, M. Forejt<sup>1)</sup>

<sup>1)</sup> Brno University of Technology, Faculty of Mechanical Engineering, Czech Republic

Received: 07.08.2012

Accepted: 12.09.2012

\*Corresponding author: e-mail: miroslav.slais@gmail.com, Tel.: +420 541 142 613, Department of Metal Forming and Plastics, Faculty of Mechanical Engineering, Brno University of Technology, Technická 2896/2, 616 69 Brno, Czech Republic

### Abstract

The paper deals with the influence of strain rate on the mechanical behaviour of the Ti-6Al-4V titanium alloy. After verification tests under static loading conditions, the specimens were deformed at high strain rates using the device for the Taylor anvil test. Results of an image analysis of deformed specimens from the Taylor anvil test were used as a reference for the comparison of experiment and computer simulation in the ANSYS LS-DYNA 3D program. Using a new developed algorithm the parameters of Johnson-Cook equation were determined to obtain the best possible agreement between deformed shapes obtained by numerical simulation and by real experiment.

**Keywords:** finite element modeling, constitutive equations, titanium alloys

### 1 Introduction

Most simulation programs use the finite element method, where a continuous area is meshed into a set of discrete sub-areas. There are countless types of elements with different numbers of degrees of freedom, which are suitable for modelling various forming operations [1-3]. Common simulation programs for metal forming are not suitable to simulate dynamic loading, because they consider quasi-static conditions and are unable to take into account the influence of inertial forces [4-5]. Since the strain rate is high for the Taylor anvil test (up to  $10^4 \text{ s}^{-1}$ ), it is necessary to simulate this experiment using the program for numerical simulation of highly nonlinear dynamical processes (e.g. PAM CRASH, LS-DYNA) [6-7].

LS-DYNA is multi-functional simulation software for the analysis of strongly nonlinear physical processes with large deformations that occur in a short time [8]. The problems of crash simulation tests in automotive technology can be given as an example. The program is characterized by fully automatic generation of contacts, more than 130 material models and algorithms for the simulation of forming processes (adaptive mesh) [9-10].

There are number of material models that appropriately describe the actual course of deformation stress – the strain dependence. Some models are valid only under static loading conditions, others can be used in a wide range of strain rates and some models reflect the influence of temperature. The Johnson-Cook equation (1.) is one of those models, which are often used for materials with the BCC lattice and has 5 parameters that are determined experimentally. This constitutive relationship is very often used because it is able to cover with a few parameters a very wide range of the influence of temperature and strain rate on deformation stress [11-16].

$$\sigma = \sigma_0 + B \cdot \varepsilon^n \left( 1 + C \cdot \ln \frac{\dot{\varepsilon}}{\dot{\varepsilon}_0} \right) \left[ 1 - (T^*)^m \right] \quad (1.)$$

where:  $\sigma_0$  [MPa] - the yield stress  
 $B$  [MPa] - the hardening modulus  
 $C$  [-] - the strain rate sensitivity coefficient  
 $n$  [-] - the hardening coefficient  
 $m$  [-] - the thermal softening coefficient  
 $T^*$  [-] - the normalized temperature  
 $\dot{\varepsilon}_0$  [ $s^{-1}$ ] - the referential strain rate (most frequently it is equal to  $1 s^{-1}$ )

## 2 Experimental material and methods

The Ti-6Al-4V titanium alloy was chosen for the experiments. This alloy is known as a 'workhorse' of the titanium industry because its production amounts to as much as 50% of the total production of titanium alloys. It is an  $\alpha+\beta$  alloy that can be heat-treated to achieve moderate increases in strength. The Ti-6Al-4V is recommended for use at operating temperatures of up to approximately 350°C. It offers a combination of high strength, light weight, formability and corrosion resistance [17-19].

The Taylor anvil test [20-21] is one of the material tests where strain rates up to  $10^4 s^{-1}$  can be achieved at relatively low impact speed of the test specimen. In the test a cylindrical specimen is accelerated against a hard surface (measuring bar). The specimen 25 mm in length and 5 mm in diameter is placed into a support (usually made of polystyrene) and then accelerated by expanding air in a gas gun towards the impact chamber. The specimen is separated from the support before its impact on the measuring bar [22].

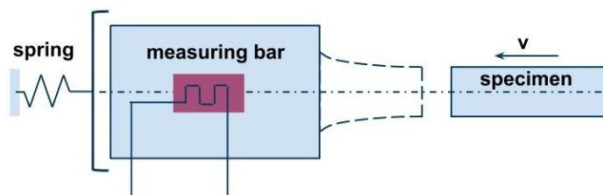


**Fig. 1** Principle of the Taylor anvil test

Since the specimen deforms into a "funnel" shape after the impact (see **Fig. 1**), it is not possible to get all the dimensions using currently available gauges. The Lucia software for image analysis is used to determine exact geometry of the deformed specimen. The program works in conjunction with a CCD zoom camera. The scanned specimen contour (see **Fig. 2**) is then processed in MS Excel and it is compared with the results of numerical simulations.

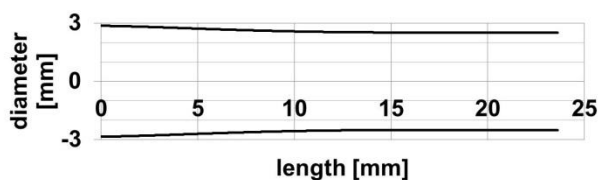


**Fig. 2** Ti-08 specimen contour ( $v = 220$  m/s)

### 3 Results

Modelling of the Taylor anvil test consists in setting and searching for suitable parameters that best describe the equation (1.) is used because of the low time demands of the numerical simulation. The results of numerical simulation of the Taylor anvil test are compared with actual results obtained in the experiment. The main criterion is to achieve the best possible correspondence of deformed shapes. The parameters thus obtained are valid only for a clearly defined chemical composition of the material and its heat treatment (in our case for the Ti-6Al-4V alloy, annealed at 715°C for 1.5 hours).

A new algorithm was developed based on previous numerical simulations. Its function is to set the parameters of constitutive equation as best as possible. The impact speed and initial geometry of the specimen are set into the algorithm as well as intervals for particular parameters of the Johnson-Cook equation. Parameters for the primary simulations were set on the basis of static upsetting tests and parameters identified from the literature (see **Table 1**). Subsequent cycling changes the values of parameters ( $\sigma_0$ , B, C, n, m) according to inputs and writes out selected dimensions of the deformed shape geometry, as shown in **Fig. 3**.

**Table 1** Parameters of Johnson-Cook equation [23-24]

$\sigma_0$ [MPa]	B [MPa]	C [-]	n [-]	m [-]
862	331	0.012	0.34	0.8
870	990	0.011	0.45	1.0
1 048	950	0.015	0.20	1.0

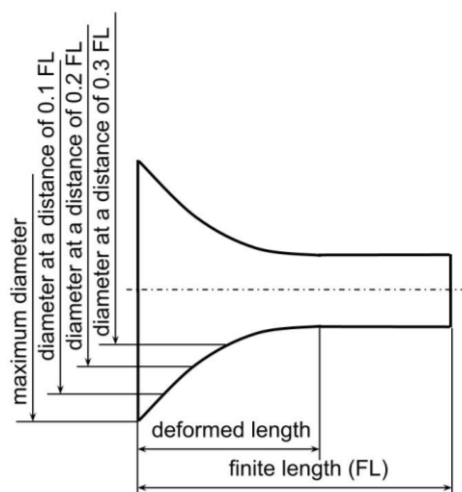


**Fig. 3** Parameters determined by algorithm

The output is a text file where the values of specific constitutive equation parameters are matched with specific parameters of the deformed shape. This file is further processed in MS Excel, where a shape closest to reality is selected via filtering.

Another step to improve the accuracy of determining the parameters would be to create a neural network that would set the parameters of constitutive equations based on the basis of the input conditions of the experiment. The following simplifications have been used to reduce the time demands of the simulation:

- The specimen impacts perpendicularly on the bar.
- The bar is ideally rigid and there is no plastic deformation after the impact.
- The solution is in the axial cross-section (2D).
- The simulation solves only one half of the axial cross-section, so it uses axial symmetry.

The best parameters of the Johnson-Cook equation were determined using numerical simulations and are shown in **Table 2**. The static yield stress was determined from upsetting tests. Previously obtained stress - strain curves in the temperature range of 20 to 500°C were used for a correct determination of the m parameter. The split Hopkinson pressure bar test (SHPBT) was used to obtain these curves [18]. The m exponent was determined such that the stress values for a particular temperature and medium strain rate calculated by Johnson-Cook equation correspond with the values from SHPBT as shown in **Fig. 4**.

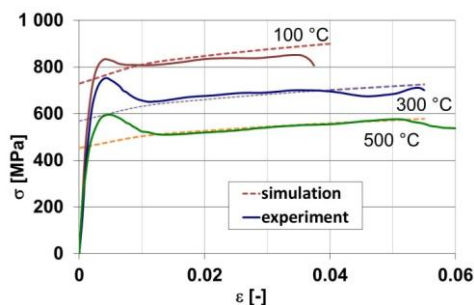


**Fig. 4** Comparison of stress-strain curves from Split Hopkinson pressure bar test and calculated using Johnson-Cook equation

**Table 2** Parameters of Johnson-Cook equation determined by numerical simulation

$\sigma_0$ [MPa]	B [MPa]	C [-]	n [-]	m [-]
802	995	0.010	0.50	0.60

**Table 3** Comparison of actual and calculated dimensions for selected specimens

Specimen		Ti-19	Ti-13	Ti-12	Ti-9	Ti-27
Impact speed [m/s]		100	170	195	210	220
Finite length [mm]	actual	24.80	24.26	24.03	23.81	23.67
	simulation	24.52	23.70	23.33	23.10	22.93
	error	-1.13 %	-2.38 %	-2.99 %	-3.09 %	-3.22 %
Diameter at a distance of 0.1 FL [mm]	actual	5.18	5.35	5.45	5.45	5.56
	simulation	5.22	5.46	5.57	5.63	5.68
	error	0.77 %	1.99 %	2.07 %	3.25 %	2.07 %
Diameter at a distance of 0.2 FL [mm]	actual	5.09	5.29	5.40	5.34	5.39
	simulation	5.17	5.31	5.40	5.45	5.49
	error	1.57 %	0.44 %	0.00 %	2.10 %	1.83 %
Diameter at a distance of 0.3 FL [mm]	actual	5.10	5.12	5.12	5.12	5.17
	simulation	5.13	5.16	5.21	5.24	5.27
	error	0.59 %	0.78 %	1.80 %	2.38 %	1.81 %
Length of the nondeformed end [mm]	actual	18.34	16.17	14.40	14.50	14.34
	simulation	18.63	15.29	14.66	14.31	14.00
	error	1.56 %	-5.75 %	1.77 %	-1.34 %	-2.40 %

The following table shows the percentage error between actual dimension and dimension calculated by numerical simulation. The actual dimension is considered to be 100 percent. Geometry parameters were compared for specimens Ti - 9, 12, 13, 19 and 27 where each specimen represents one area in the interval of actual impact speeds. The agreement of the results is  $\pm 5\%$  and the parameters of constitutive equations thus established can be considered representative.

### 3.1 Results of numerical simulation for the Ti-12 specimen

**Fig. 5** shows a comparison of deformed shape between simulation and experiment for the Ti-12 specimen. The impact speed was 194.9 m/s. The maximum diameter mismatch is caused by the physical laws that cannot be fully taken into account in numerical simulation. Other values of effective stress and strain according to the HMH condition are shown in **Figs. 6** and **7**.

The final specimen shape is given by the arrangement of the Taylor anvil test, and therefore the maximum strain and stress occur at the specimen front, which impacts on the rigid bar.

During the Taylor anvil test the strain rate is not constant over the entire specimen length. The highest strain rate is at the deformed front of the specimen and gradually falls to zero (boundary of the deformed and the non-deformed part of the specimen). The maximum strain rate was from about  $4\,000\text{ s}^{-1}$  for the Ti-19 specimen to  $8\,800\text{ s}^{-1}$  for the Ti-27 specimen.

Contour correspondence is searched for in areas with the strain rate in the order of about  $10^3\text{ s}^{-1}$ , i.e. is about 2 mm from the deformed end. Simulation and experiment results show very good agreement in this range of specimen lengths.

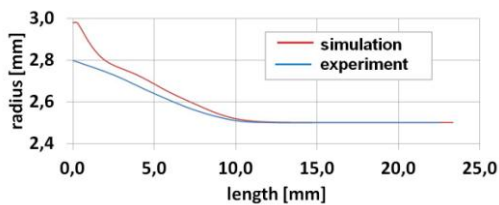


**Fig. 5** Comparison of deformed shape between simulation and experiment

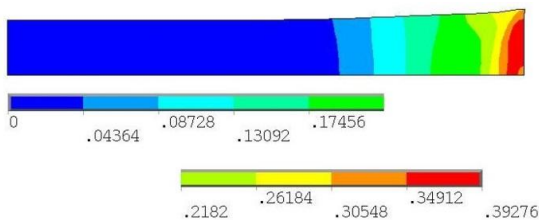


**Fig. 6** Resultant engineering strain for the Ti-12 specimen

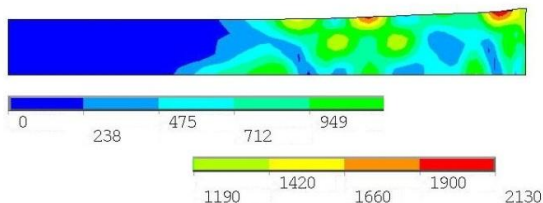


**Fig. 7** Resultant effective stress [MPa] for the Ti-12 specimen

#### 4 Discussion

Due to simplicity and availability of material coefficients many numerical simulations are based on the Johnson–Cook material model. On the other hand, the Johnson–Cook model might lead to questionable results in the high-dynamic region [25]. This model also exhibits unrealistically small strain-rate dependence at high temperatures [26]. Since the strain rate was in the order of  $10^3 \text{ s}^{-1}$  and temperature below the recrystallization temperature we can assume that Johnson–Cook equation predicts mechanical material behaviour for studied thermomechanical conditions well enough.

Number and type of elements affect time needed to solve the simulation of the Taylor anvil test. Eight-node 3D solid elements with one-point integration and stiffness-based hourglass control can be used to discretize the cylindrical specimens [25]. In order to reduce CPU cost of simulations, a quarter of the Taylor cylinder is very often generated using a uniform mesh [27]. We used a 2D solid element and axisymmetric method for solving time reduction. The use of 2D element in comparison with 3D element has no significant effect on the accuracy of simulation results [28, 29].

According to equation (1.) there is a set of five model parameters that need to be identified. This is normally done through inverse identification method. Other strategy is to find the strain hardening related parameters from a quasi-static test and thermal softening parameter from experiments at different temperatures but identical strain rate [15]. In our case the yield stress was obtained from quasi-static upsetting test. Other parameters were determined using a new developed algorithm. This algorithm writes out selected dimensions of the deformed shape geometry according to a set of model parameters. The advantage of this method is quick and accurate determination of Johnson-Cook equation parameters.

#### 5 Conclusion

The aim of this paper was to introduce a potential method for the determination of five parameters of the Johnson-Cook constitutive equation for the Ti-6Al-4V titanium alloy. The Johnson-Cook equation parameters were established using numerical simulation in the LS DYNA 3D software and the Taylor anvil test facility that is located in the High strain rate laboratory at the FME BUT. The results of image analysis of deformed specimens from the Taylor anvil test are used for a comparison of experiment to numerical simulations. The parameters of the Johnson-Cook equation were determined using an algorithm so that they represent the actual specimen contour from the physical experiment as accurately as possible. The agreement of specimen shapes between physical experiment and numerical simulation is  $\pm 5\%$ .

The parameters obtained for the Ti-6Al-4V titanium alloy (annealed at  $715^\circ\text{C}$  for 1.5 hours) are  $\sigma_0 = 802\text{MPa}$ ,  $B = 995\text{MPa}$ ,  $C = 0.01$ ,  $n = 0.50$ ,  $m = 0.60$ . These parameters are valid for the calculation of the material dynamic yield stress for strain rates up to  $1000 \text{ s}^{-1}$  and temperatures of 20 to  $500^\circ\text{C}$ . The value of dynamic yield stress is applied in programs where forming does not occur under quasi-static but dynamic loading conditions.

#### References

- [1] S. K. Panthi, N. Ramakrishnan, K.K. Pathak, J.S. Chouhan: Journal of Materials Processing Technology, Vol. 186, 2007, No. 1-3, p. 120-124

- [2] M. Kawka, T. Kakita, A. Makinouchi: *Journal of Materials Processing Technology*, Vol. 80-81, 1998, p. 54-59
- [3] A. Makinouchi, C. Teodosiu, T. Nakagawa: *CIRP Annals - Manufacturing Technology*, Vol. 47, 1998. No. 2, p. 641-649
- [4] C.L. Chow, W.H. Tai, Edmund Chu: *Journal of Materials Processing Technology*, Vol. 139, 2003, No. 1-3, p. 553-558
- [5] Recep Gümrtük, Sami Karadeniz: *International Journal of Mechanical Sciences*, Vol. 51, 2009, No. 5, p. 350-362
- [6] Michael Brüning, Larissa Driemeier: *International Journal of Plasticity*, Vol. 23, 2007, No. 12, p. 1979-2003
- [7] Kee Poong Kim, Hoon Huh: *International Journal of Solids and Structures*, Vol. 43, 2006, No. 21, p. 6488-6501
- [8] Q. Zhang, T.A. Dean, Z.R. Wang: *International Journal of Machine Tools and Manufacture*, Vol. 46, 2006, No. 7-8, p. 699-707
- [9] A.G. Hanssen, Y. Girard, L. Olovsson, T. Berstad, M. Langseth: *International Journal of Impact Engineering*, Vol. 32, 2006, No. 7, p. 1127-1144
- [10] T. Børvik, O.S. Hopperstad, T. Berstad, M. Langseth: *International Journal of Impact Engineering*, Vol. 27, 2002, No. 1, p. 37-64
- [11] M. A. Meyers: *Dynamic Behaviour of Materials*, John Wiley & Sons, New York, 1994
- [12] H. E. Konokman, M. M. Çoruh, Altan Kayran: *Acta Mechanica*, Vol. 220, 2011, No. 1-4, p. 61-85
- [13] W. K. Rule: *International Journal of Impact Engineering*, Vol. 19, 1997, No. 9-10, p. 797-810
- [14] J. Nussbaum, N. Faderl: *Procedia Engineering*, Vol. 10, 2011, p. 3453-3458
- [15] A. S. Milani, et al.: *International Journal of Impact Engineering*, Vol. 36, 2009, p. 294-302
- [16] J. Buchar, M. Forejt, M. Jopek, I. Křivánek: *Journal dePhysique*, Vol. IV, 2000, p. Pr9-75-Pr9-80
- [17] G. Luetjering, J. C. Williams: *Titanium*. Springer-Verlag, Heidelberg, 2003
- [18] M. Šlais, M. Forejt: *Steel Research International*, Vol. 2, 2008, p. 693-697
- [19] S. Ashely: *Mechanical Engineering*, Vol. 115, 1993, No. 7, p. 60-65.
- [20] S. E. Jones, J. A. Drinkard, W. K. Rule, L. L. Wilson: *International Journal of Impact Engineering*, Vol. 21, 1998, No. 1-2, p. 1-13
- [21] M. Šlais, M. Knebl, M. Forejt: *MM Science Journal*, Vol. 4, 2010, p. 214-216
- [22] J. E. Field, et al.: *International Journal of Impact Engineering*, Vol. 30, 2004, p. 109-177
- [23] J. Buchar, J. Voldřich: *Terminal ballistics*, first ed., Academia, Praha, 2003 (in Czech)
- [24] D. Umbrello, D., R. M'Saoubi, J. C. Outeiro: *International Journal of Machine Tools and Manufacture*, Vol. 47, 2007, No. 3-4, p. 462-470
- [25] M. Brüning a, L. Driemeier: *International Journal of Plasticity*, Vol. 23, 2007, No. 12, p. 1979-2003
- [26] [5.5.2012], <http://www.scribd.com/doc/80985178/Biswajit-Banerjee-An-evaluation-of-plastic-flow-stress-models-for-the-simulation-of-high-temperature-and-high-strain-rate-deformation-of-metals>, B. Banerjee: *An evaluation of plastic flow stress models for the simulation of high-temperature and high-strain-rate deformation of metals*
- [27] R. Vignjevic, N. Djordjevic, J. Campbell, V. Panov: *International Journal of Impact Engineering*, Vol. 49, 2012, p. 61-76

- [28] H. E. Konokman, M. M. Çoruh, A. Kayran: Acta Mechanica, Vol. 220, 2011, No. 1-4, p. 61-85
- [29] J. L. Cantero, C. Santiuste, N. Marín, X. Soldani, H. Miguélez: AIP Conference Proceedings, Vol. 1431, 2012, No.1, p. 651-659

### **Acknowledgements**

*Authors are grateful for the support of experimental works by projects FSI-S-11-26 Using of Advancement Technologies in Production of Heat Transfer Solar Panels and FSI-J-12-1818.*